

## Article

# Improved Viability of Probiotics via Microencapsulation in Whey-Protein-Isolate-Octenyl-Succinic-Anhydride-Starch-Complex Coacervates

Qingqing Liu <sup>1,2</sup> , Chutian Lin <sup>1,2</sup>, Xue Yang <sup>1,2</sup>, Shuwen Wang <sup>1,2</sup>, Yunting Yang <sup>1,2</sup>, Yanting Liu <sup>1,2</sup>, Mingming Xiong <sup>1,2</sup>, Yisha Xie <sup>1,2</sup>, Qingbin Bao <sup>1,2,\*</sup> and Yongjun Yuan <sup>1,2,\*</sup>

- <sup>1</sup> Chongqing Key Laboratory of Speciality Food Co-Built by Sichuan and Chongqing, School of Food and Bioengineering, Xihua University, Chengdu 610039, China; liuqing\_861006@163.com (Q.L.)
- <sup>2</sup> Key Laboratory of Grain and Oil Processing and Food Safety of Sichuan Province, College of Food and Bioengineering, Xihua University, Chengdu 610039, China
- \* Correspondence: bao717@126.com (Q.B.); yyja9791@sina.com (Y.Y.); Tel.: +86-138-0818-3804 (Q.B.); +86-139-8225-9820 (Y.Y.)

**Abstract:** The aim of this study was to microencapsulate probiotic bacteria (*Lactobacillus acidophilus* 11073) using whey-protein-isolate (WPI)–octenyl-succinic-anhydride-starch (OSA-starch)-complex coacervates and to investigate the effects on probiotic bacterial viability during spray drying, simulated gastrointestinal digestion, thermal treatment and long-term storage. The optimum mixing ratio and pH for the preparation of WPI-OSA-starch-complex coacervates were determined to be 2:1 and 4.0, respectively. The combination of WPI and OSA starch under these conditions produced microcapsules with smoother surfaces and more compact structures than WPI-OSA starch alone, due to the electrostatic attraction between WPI and OSA starch. As a result, WPI-OSA-starch microcapsules showed significantly ( $p < 0.05$ ) higher viability ( $95.94 \pm 1.64\%$ ) after spray drying and significantly ( $p < 0.05$ ) better protection during simulated gastrointestinal digestion, heating ( $65\text{ °C}/30\text{ min}$  and  $75\text{ °C}/10\text{ min}$ ) and storage ( $4/25\text{ °C}$  for 12 weeks) than WPI-OSA-starch microcapsules. These results demonstrated that WPI-OSA-starch-complex coacervates have excellent potential as a novel wall material for probiotic microencapsulation.

**Keywords:** probiotic; microencapsulation; whey-protein isolate; octenyl-succinic-anhydride starch; complex coacervation



**Citation:** Liu, Q.; Lin, C.; Yang, X.; Wang, S.; Yang, Y.; Liu, Y.; Xiong, M.; Xie, Y.; Bao, Q.; Yuan, Y. Improved Viability of Probiotics via Microencapsulation in Whey-Protein-Isolate-Octenyl-Succinic-Anhydride-Starch-Complex Coacervates. *Molecules* **2023**, *28*, 5732. <https://doi.org/10.3390/molecules28155732>

Academic Editor: Leslaw Juszcak

Received: 23 June 2023

Revised: 18 July 2023

Accepted: 26 July 2023

Published: 28 July 2023



**Copyright:** © 2023 by the authors. Licensee MDPI, Basel, Switzerland. This article is an open access article distributed under the terms and conditions of the Creative Commons Attribution (CC BY) license (<https://creativecommons.org/licenses/by/4.0/>).

## 1. Introduction

Probiotics are living microorganisms that can provide a lot of benefits to the health of a host when properly ingested [1,2]. Many probiotics, including *Bifidobacterium*, *Lactobacillus* and others, have been widely used in functional foods, beverages and so on [1,3]. However, the instability of probiotics during food processing, human gastrointestinal digestion, long-term storage and more is still a great challenge [4,5]. Microencapsulation is considered to be an effective method to provide physical protection, and thereby increase the viability of probiotics [6]. Among the various microencapsulation methods, spray drying is considered to be one of the most widely used methods due to its moderate price, ease of operation, continuous production and excellent safety [7].

It is universally acknowledged that the choice of wall materials is of great importance for microencapsulation [8]. For the microencapsulation of probiotics, proteins and polysaccharides are the most commonly used wall materials [9]. Proteins have good film-forming properties, but are easily degraded by pepsin in gastric fluids and have a tendency to aggregate [10]. Polysaccharides can maintain their stability in the stomach due to their good resistance to acid and pepsin, which can improve the compactness of the microcapsules

and be beneficial for the targeted release of probiotics. On the other hand, polysaccharides generally cannot provide adequate protection for probiotics due to their poor film-forming properties and the large pores between their molecular chains [11]. Therefore, compared to protein/polysaccharide alone, the probiotic microcapsules with higher encapsulation viability and more stability could be prepared by the combination of them [10,11].

Whey-protein isolate (WPI), isolated from cheese-making waste, is an attractive encapsulant as it has been found to be effective in protecting probiotic bacteria during spray drying [12]. However, WPI cannot provide an effective moisture barrier and therefore cannot effectively protect probiotics during storage due to its hydrophilic nature [12,13]. Octenyl succinic anhydride (OSA) starch, i.e., starch modified with OSA groups (an esterifying agent), has been recognised as a safe polysaccharide by the United States Food and Drug Administration (FDA) [7,14]. The hydrophobicity of OSA starch is relatively high with a contact angle of about 80° due to the presence of lipophilic octenyl groups [15,16]. In addition, the digestibility of OSA starch was relatively low due to the spatial obstruction caused by the OSA groups, which reduces its contact with digestive enzymes [17]. According to Wang et al., the relatively high hydrophobicity (contact angle of 76.10°) and digestion resistance of modified starch (propionylated potato starch) was beneficial in protecting probiotics during spray drying, simulated gastrointestinal (SGI) digestion and storage [18]. OSA starch alone cannot provide sufficient protection for probiotics during spray drying. As reported by Cruz-Benítez et al. [19], the viability of *Lactobacillus pentosus* in OSA starch microcapsules after spray drying was only about 65%. The weak protective effect of the OSA starch microcapsules could be attributed to the poor solubility and film-forming property of OSA starch, resulting in an uneven film formation at the beginning of the drying process and therefore the shrunken and wrinkled surfaces of the spray-dried microcapsules [19,20].

Complex coacervation is one of the most commonly used methods for combining protein with polysaccharide, which occurs as a phase separation of the water solution containing them with opposite electrical charges and the formation of a coacervate layer surrounding the bioactive compound [21]. Probiotic microcapsules formed via complex coacervation have advantages in encapsulation viability, protective capability, controlled release, etc. [9]. To date, complex coacervates of pea-protein isolate–sugar-beet pectin, sodium caseinate–sugar-beet pectin, soy-protein isolate–pectin, soy-protein isolate–peach-gum polysaccharide, WPI–gum arabic, soy-protein isolate–carrageenan, casein–chitosan and others have been used for probiotic microencapsulation [9,10,21–23]. However, the use of WPI–OSA–starch–complex coacervates in probiotic microencapsulation has not been reported. Therefore, in the present study, WPI–OSA–starch–complex coacervates were used as the wall material for *Lactobacillus acidophilus* encapsulation via spray drying. The SGI digestion, thermal resistance and storage properties of microencapsulated and free probiotic bacteria and the physicochemical properties and microstructure of probiotic microcapsules were further investigated.

## 2. Results and Discussion

### 2.1. Formation of WPI–OSA–Starch–Complex Coacervates

#### 2.1.1. Turbidity

Complex coacervation of charged protein and polysaccharide can be reflected by the change in turbidity of the solution at the macroscopic level. Therefore, turbidity titration has usually been used to investigate the whole process of complex coacervation and to measure the conditions under which the maximum complex coacervates can be formed [24].

As shown in Figure 1a, the turbidity of the WPI–OSA–starch mixtures increased firstly and then decreased as the pH lowered from 2.0 to 6.5. The pH<sub>opt</sub> was determined to be 3.8, 3.9, 4.0 and 4.1 when the mixing ratios were 0.5:1, 1:1, 2:1 and 3:1, respectively. These results indicated that an increase in WPI in the mixture required an increase in the pH<sub>opt</sub>, similar to the report of Qiu et al. [25] and Tian et al. [26]. In addition, the maximum turbidity value was significantly influenced by the mixing ratio. As the mixing ratio of

WPI-OSA starch was 0.5:1, i.e., the amount of WPI was lower than that of OSA starch, only weak interactions occurred between WPI and OSA starch, resulting in relatively low turbidity. Similar phenomena have also been reported for other combinations of protein polysaccharide, such as hemp-protein isolate–gum arabic, gelatin–OSA-modified kudzu starch and others [27,28]. The reason for this can be attributed to there being too many anionic groups in the polysaccharide, resulting in strong electrostatic repulsion between them. As the mixing ratio increased, the turbidity first increased and then decreased. The highest turbidity was observed when the WPI-OSA starch ratio was 2:1 and the pH was 4.0, indicating the formation of WPI-OSA-starch complex coacervates with maximum insolubility and stability. Similar phenomena were also observed by Plati et al. [27] and Tian et al. [26]. Thus, this is the possible optimum mixing ratio for the correct saturation of the charged sites of the OSA with WPI molecules [27]. Turbidity decreased when the ratio was further increased to 3:1; this was also in agreement with the report of Plati et al. [27] and Tian et al. [26] and could be attributed to an excess of WPI in the solution, which could not bind to the OSA starch, being replaced by protein self-aggregation [27]. This assumption was supported by a shift of pH<sub>opt</sub> closer to the PI of WPI.

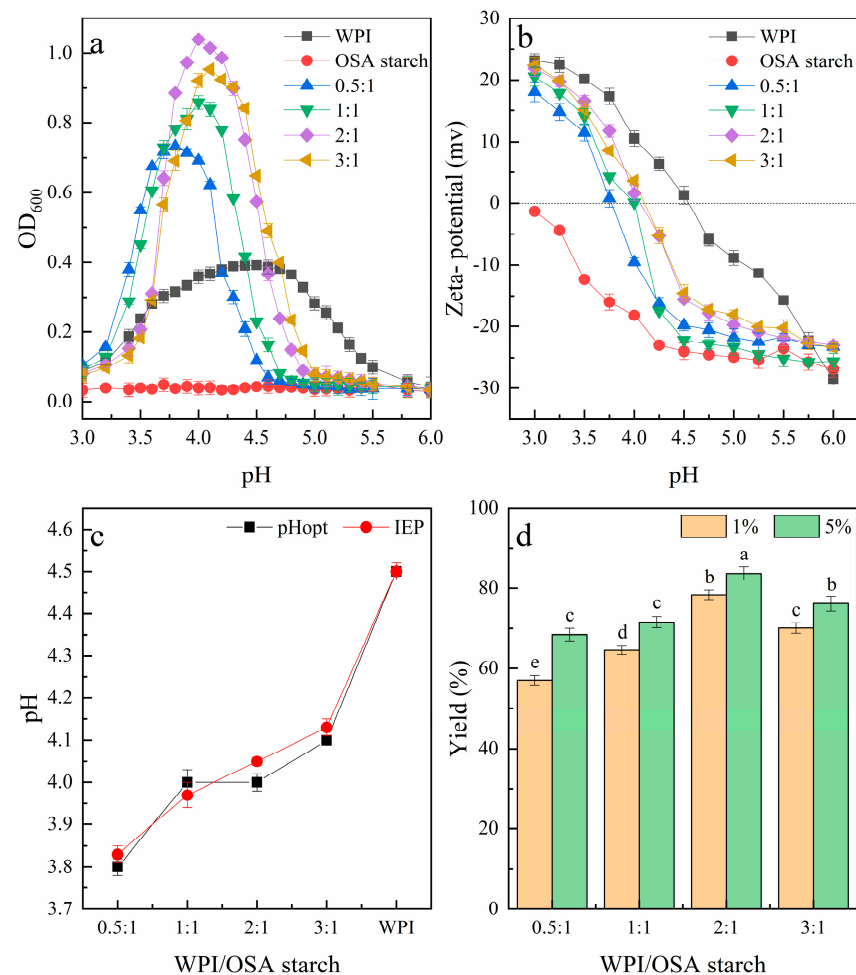


**Figure 1.** Effects of mixing ratio, pH and total polymer concentration on the formation of WPI-OSA-starch-complex coacervates. (a) Zeta potential and (b) turbidity of WPI-OSA starch alone and WPI-OSA starch mixtures at different ratios as a function of pH; (c) the pH<sub>opt</sub> and IEP of WPI-OSA-starch mixtures at different ratios; (d) the yield of WPI-OSA-starch-complex coacervates at different ratios and different total polymer concentrations. Different lowercase letters in (d) mean significant differences ( $p < 0.05$ ).

### 2.1.2. Zeta Potential

As the complex coacervation of protein and polysaccharide is mainly motivated by electrostatic attraction, their zeta potential could provide important information about the interaction between them, as well as the formation and stability of complex coacervates [29].

As shown in Figure 1b, the zeta potential of the WPI decreased with increasing pH from 3.0 to 6.0 and changed from positive to negative at about pH 4.5, which is its IEP, similar to the previous report [30]. In contrast, OSA starch mainly maintained a negative charge and decreased with increasing pH from 3.0 to 6.0, which is similar to the previous report of Zhao et al. [28]. The zeta potential of all the WPI-OSA-starch blends was intermediate between the two single biopolymers. The IEP was found to be 3.83 at a mixing ratio of 0.5:1 (WPI-OSA starch). When the mixing ratio of WPI-OSA starch was increased from 0.5:1 to 3:1, the IEP values also increased, reaching a maximum of 4.13 at a mixing ratio of 3:1 (Figure 1b). Similar phenomena have been observed previously for other combinations of protein polysaccharide, e.g., hemp-protein isolate–gum arabic, pea-protein isolate–beet pectin and others [27,29].

### 2.1.3. Comparison of IEP and pH<sub>opt</sub>

As shown in Figure 1c, the pH<sub>opt</sub> determined via turbidimetric analysis at each mixing ratio approximately coincided with the IEP. This phenomenon is consistent with the previous reports that the maximum turbidity of the mixed solutions of protein polysaccharide is generally observed at their IEP [27,31,32], confirming again that electrostatic interaction is the main driving force for the complex coacervation.

### 2.1.4. Yield of Complex Coacervates

As shown in Figure 1d, at a total polymer concentration of 1%, the yield of the complex coacervates increased with increasing WPI-OSA-starch-mixing ratio and the highest amount of complex coacervates ( $78.33 \pm 2.24\%$ ) was formed when the WPI-OSA-starch-mixing ratio was 2:1, which corresponded to the highest turbidity. A similar yield of complex coacervates has also been obtained for other systems, such as WPI–quince-seed mucilage, soybean-protein isolate–soluble dietary fiber of Sichuan pepper seed and others [31,33]. However, as the mixing ratio was further increased, the yield of the complex coacervates started to decrease, which was attributed to the fact that the excess WPI was unable to bind with the OSA starch and remained soluble in the equilibrium phase [34]. In addition, the yield of WPI-OSA-starch-complex coacervates increased to  $83.73 \pm 2.75\%$  as the total biopolymer concentration increased to 5%, similar to the report of Bhargavi et al. [35]. The reason for this can be attributed to the increased number of charged sites available for electrostatic interaction at a high biopolymer concentration [35].

Therefore, the conditions for the preparation of WPI-OSA-starch-complex coacervates for probiotic encapsulation were selected as follows: mixing ratio 2:1, pH 4.0, total polymer concentration of 5%.

## 2.2. FTIR Spectroscopy

Figure 2 shows the FTIR spectroscopy of probiotic microcapsules. For WPI microcapsules, it is noticeable that the peaks at  $1645\text{ cm}^{-1}$ ,  $1539\text{ cm}^{-1}$  and  $1240\text{ cm}^{-1}$  were related to the amide I (C=O stretching), amide II (N-H bending) and amide III (C-N stretching and N-H deformation) of WPI, respectively [36]. For OSA-starch microcapsules, the peak at  $3000\text{--}3500\text{ cm}^{-1}$  was related to the O-H stretching of hydroxyl groups. The peaks at  $1725$  and  $1572\text{ cm}^{-1}$  were observed for the stretching vibration of C=O and asymmetric stretching of  $\text{COO}^-$ , respectively [37]. The FTIR spectrum of WPI-OSA-starch microcapsules was the combination of the FTIR spectrum of WPI microcapsules and OSA-starch microcapsules, although the location of the peaks was slightly changed, consistent with the report of Naderi et al. [38] and Zhang et al. [39]. In addition, the peaks shifted from  $1645\text{ cm}^{-1}$  and  $1539\text{ cm}^{-1}$  in the WPI microcapsules to  $1650\text{ cm}^{-1}$  and  $1544\text{ cm}^{-1}$  in the WPI-OSA-starch microcapsules, respectively, similar to the report of Naderi et al. [38] and Zhang et al. [39].

Furthermore, the peaks of OSA starch at  $1725\text{ cm}^{-1}$  and  $1571\text{ cm}^{-1}$  disappeared in the WPI-OSA-starch microcapsules, similar to the report of Zhao et al. [28]. The above changes confirmed the electrostatic attraction between the carboxyl groups ( $-\text{COO}^-$ ) of OSA starch and the amine groups ( $-\text{NH}_3^+$ ) of WPI.

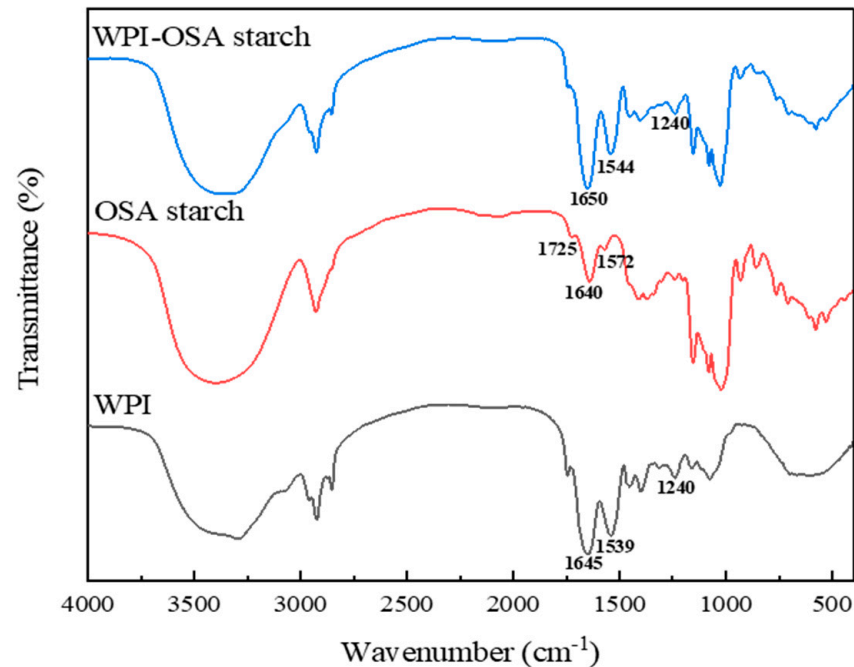


**Figure 2.** FTIR spectrogram of WPI microcapsules, OSA-starch microcapsules and WPI-OSA-starch microcapsules.

### 2.3. Microscopic Observations of Microcapsules Containing Probiotics

Fluorescence microscopy was used to confirm the presence of probiotic bacteria in the microcapsules. As shown in Figure 3a, after labelling with RBITC, free probiotic bacteria can be seen in red under the fluorescence microscope, similar to the report by Peñalva et al. [23]. Although there is some overlap, the encapsulation of probiotic bacteria in WPI, OSA-starch and WPI-OSA-starch microcapsules can still be confirmed by the presence of red fluorescence in all microcapsules (Figure 3b–d).

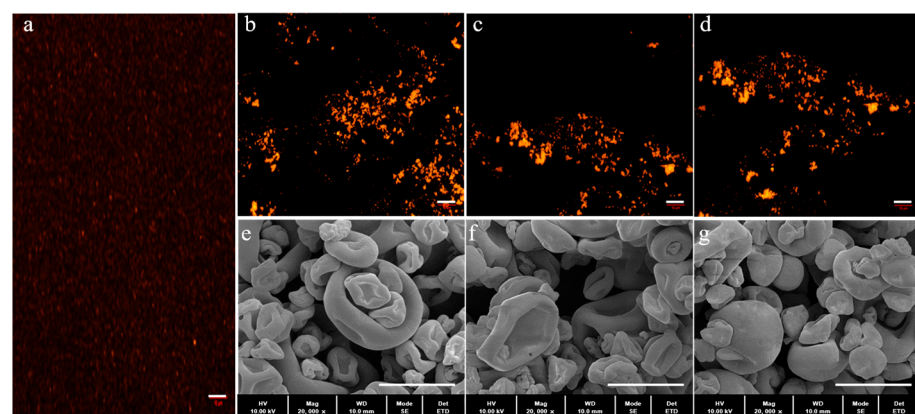


**Figure 3.** Fluorescence microscopy image of (a) aqueous suspension, (b) WPI microcapsules, (c) OSA-starch microcapsules, (d) WPI-OSA-starch microcapsules containing probiotic bacteria labelled with RBITC and SEM image of (e) WPI microcapsules, (f) OSA-starch microcapsules, (g) WPI-OSA-starch microcapsules. The bars in the fluorescence images and SEM images represent  $10\text{ }\mu\text{m}$  and  $5\text{ }\mu\text{m}$ , respectively.

The microstructure of the spray-dried microcapsules containing probiotics is also shown in Figure 3e–g. The sizes of the three microcapsules showed almost no difference. Some hollows and wrinkles were observed in both WPI microcapsules and OSA-starch microcapsules, which may result from the denaturation of WPI and the shrinkage of the OSA starch, respectively, during the spray-drying process [13,20]. The combination of WPI and OSA starch produced the microcapsules with compact structures, smooth surfaces and almost no wrinkles, which can be attributed to the electrostatic attraction between WPI and OSA starch, preventing the shrinkage of OSA starch during spray drying [20]. In addition, almost no probiotic bacteria were visible on the surface of all spray-dried microcapsules, suggesting that the probiotic bacteria were embedded in the coacervate network.

#### 2.4. Probiotic Viability, Water Content and Water Activity of Spray-Dried Microcapsules

The viability of *Lactobacillus acidophilus* in different microcapsules after spray drying is shown in Table 1. The viability of microencapsulated probiotic bacteria was  $91.32 \pm 1.87\%$  and  $70.75 \pm 2.05\%$  in WPI microcapsules and OSA-starch microcapsules, respectively. The low viability of probiotics in OSA-starch microcapsules after spray drying was also reported by Cruz-Benítez et al. [19], and could be attributed to the poor solubility and poor film-forming property of OSA starch, resulting in uneven film formation at the beginning of the drying process and shrunken and wrinkled surfaces of the spray-dried microcapsules [19,20].

**Table 1.** Probiotic viability, water content and water activity of spray-dried microcapsules.

Samples	Log N <sub>0</sub> (log CFU/g)	Log N <sub>t</sub> (log CFU/g)	Viability Log N <sub>t</sub> /Log N <sub>0</sub> (%)	Water Content (%)	Water Activity
WPI	10.03 ± 0.11 <sup>a</sup>	9.16 ± 0.17 <sup>b</sup>	91.32 ± 1.87 <sup>b</sup>	4.43 ± 0.36 <sup>b</sup>	0.205 ± 0.009 <sup>b</sup>
OSA starch	10.05 ± 0.14 <sup>a</sup>	7.11 ± 0.19 <sup>c</sup>	70.75 ± 2.05 <sup>c</sup>	5.26 ± 0.15 <sup>a</sup>	0.247 ± 0.004 <sup>a</sup>
WPI-OSA starch	10.09 ± 0.12 <sup>a</sup>	9.68 ± 0.13 <sup>a</sup>	95.94 ± 1.64 <sup>a</sup>	4.68 ± 0.28 <sup>b</sup>	0.208 ± 0.005 <sup>b</sup>

<sup>a</sup> N<sub>0</sub> is the viability of *Lactobacillus acidophilus* used for microencapsulation; N<sub>t</sub> is the viability of *Lactobacillus acidophilus* after spray drying. <sup>b</sup> Different lowercase letters in the same column mean significant differences ( $p < 0.05$ ).

WPI-OSA-starch microcapsules exhibited a significantly ( $p < 0.05$ ) higher viability ( $95.94 \pm 1.64\%$ ) than either WPI microcapsules or OSA-starch microcapsules, indicating that the combination of WPI and OSA starch would enhance the protective effect for probiotics during the process of spray drying. The high viability of probiotic bacteria in the spray-dried WPI-OSA-starch microcapsules produced here may also be due to the smooth surfaces and the compact structures of the microcapsules [1,40]. In addition, the hydroxyl groups of OSA starch could form hydrogen bonds with the cell membrane of probiotics, effectively reducing heat damage and protecting the cell membrane from degeneration during spray drying [9]. Similarly, significantly ( $p < 0.05$ ) higher probiotic viability after spray drying was also found in soy-protein-isolate-peach-gum-polysaccharide, soy-protein-isolate-pectin, WPI-*Momordica charantia*-polysaccharide microcapsules than that in protein/polysaccharide-only microcapsules and free bacteria [9,10,41]. On the other hand, decreased encapsulation viability was reported when shellac was incorporated into WPI-based microcapsules, which could be attributed to the excessive hydrophobicity of shellac (the contact angle of shellac powder of  $152.3^\circ$ ) [13,42].

As also shown in Table 1, the water content of all probiotic microcapsules was not more than 7%, which is in line with the standard acceptance values for spray-dried products [13]. The water content of the WPI-OSA-starch microcapsules was similar to that of the WPI microcapsules, but lower than that of the OSA-starch microcapsules. Similar results would also be reported that the water content of shellac microcapsules was significantly ( $p < 0.005$ ) higher than that of WPI-shellac microcapsules and WPI microcapsules due to the low drying rate of shellac microcapsules, despite the strong hydrophobicity of shellac [13]. The

$a_w$  values were consistent with the water content, and a higher  $a_w$  ( $0.247 \pm 0.004$ ) was found in the OSA starch microcapsules than in the others.

## 2.5. Viability of Microencapsulated Probiotics under Different Conditions

### 2.5.1. SGI Digestion

As shown in Figure 4, the initial number of free *Lactobacillus acidophilus* was  $10.12 \pm 0.18$  log CFU/mL, which decreased dramatically after SGI digestion, with viability of  $4.75 \pm 0.32$  and  $2.47 \pm 0.19$  log CFU/mL after digestion in SGF and SIF, respectively. After microencapsulation, the viability of *Lactobacillus acidophilus* after SGI digestion was significantly ( $p < 0.05$ ) improved. Among all the microcapsules, the WPI-OSA-starch microcapsules showed the highest viability ( $9.16 \pm 0.15$  log CFU/g) after SGI digestion.

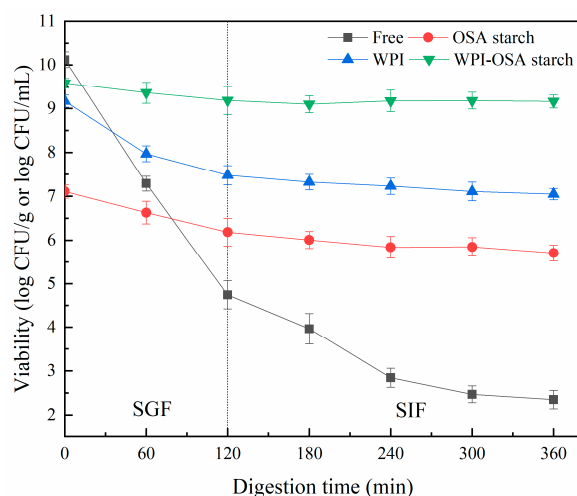


**Figure 4.** Viability of free and microencapsulated *Lactobacillus acidophilus* during simulated gastric (0–120 min) and intestinal (120–360 min) digestion.

The significant ( $p < 0.05$ ) increased viability of *Lactobacillus acidophilus* in WPI-OSA-starch microcapsules during SGI digestion could be mainly attributed to the smooth surface and the compact structure of the microcapsules, as well as the relatively high hydrophobicity of OSA starch, which were beneficial in reducing the hygroscopicity, wettability and solubility of the microcapsules and maintaining the integrity of the microcapsules during SGI digestion, thereby preventing the diffusion of hydrogen ions ( $H^+$ ), digestive enzymes, bile salts, etc., into the microcapsules [1,43,44]. In addition, the minimal damage to the probiotic bacteria in WPI-OSA microcapsules during spray drying, the ability of WPI to create a buffered microenvironment around probiotics and the resistance of OSA starch to digestion may also contribute to the improved viability of *Lactobacillus acidophilus* during SGI digestion after microencapsulation [9,18,44].

Similarly, significantly ( $p < 0.05$ ) higher probiotic viability after SGI digestion was also found in soy-protein-isolate-peach-gum-polysaccharide, soy-protein-isolate-pectin, sodium-caseinate-gum-ghatti and sodium-caseinate-gum-arabic-based microcapsules than that in protein/polysaccharide-only microcapsules and free bacteria [9,10,45]. However, sodium caseinate-maltodextrin and sodium caseinate-pullulan microcapsules were unable to protect bacterial bacteria in SGF due to the extreme solubility of maltodextrin and pullulan in aqueous media, resulting in rapid dissolution of the microparticles [45].

### 2.5.2. Heat Treatment

The influences of heat treatments on the viability of *Lactobacillus acidophilus* are shown in Figure 5. The viability of free *Lactobacillus acidophilus* rapidly decreased from  $10.07 \pm 0.13$  log CFU/mL to  $2.86 \pm 0.18$  and  $3.08 \pm 0.23$  log CFU/mL after heat treatment of  $65^\circ\text{C}/30$  min and  $75^\circ\text{C}/10$  min, respectively. After microencapsulation, the thermal

stability of *Lactobacillus acidophilus* was significantly ( $p < 0.05$ ) improved. The viability of microencapsulated *Lactobacillus acidophilus* in WPI-OSA-starch microcapsules was found to be  $8.07 \pm 0.25$  log CFU/g and  $8.52 \pm 0.19$  log CFU/g after thermal treatment of  $65^\circ\text{C}/30$  min and  $75^\circ\text{C}/10$  min, respectively, significantly ( $p < 0.05$ ) higher than that in WPI microcapsules and OSA-starch microcapsules. The reason for this could be mainly attributed to the improved sealing properties of the microcapsules due to their compact structure and smooth surface, which slows down the heat diffusion.

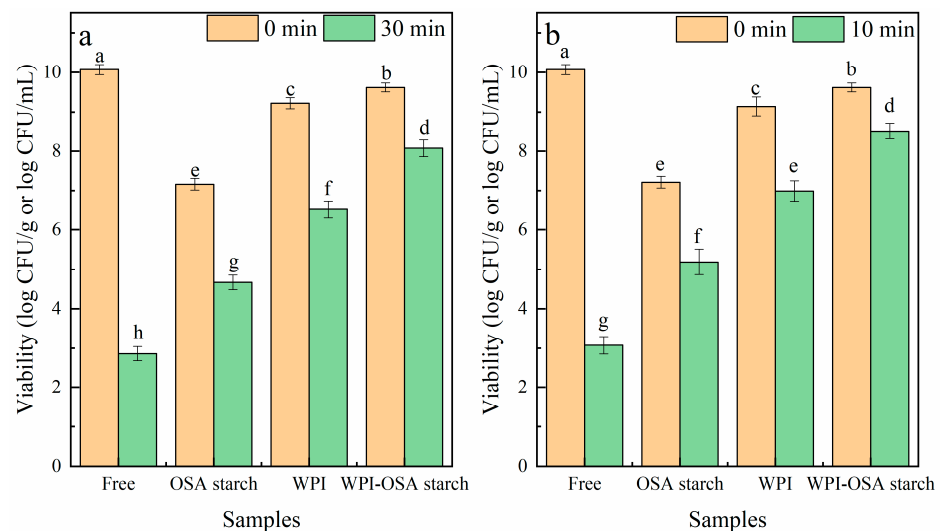


**Figure 5.** Viability of free and microencapsulated *Lactobacillus acidophilus* after thermal treatment of (a)  $65^\circ\text{C}/30$  min and (b)  $75^\circ\text{C}/10$  min. Significant differences ( $p < 0.05$ ) are indicated by different lowercase letters.

Similar results were also reported previously—the viability loss of probiotic bacteria in soy-protein-isolate-pectin microcapsules was only 2.55 log CFU/g, which was lower than that in SPI microcapsules (3.1 log CFU/g) after thermal treatment ( $75^\circ\text{C}/10$  min) [9]. However, as compared to soy-protein-isolate microcapsules, the combination of peach gum polysaccharide with soy-protein isolate reduced the viability of probiotic bacteria during the heat treatment due to the good solubility of peach-gum polysaccharide in aqueous solution, which accelerated the dissolution of the microcapsules [10]. These results suggest that the physicochemical properties of the polysaccharide are very important with respect to improving the structural compactness and thermal stability of the microcapsules.

### 2.5.3. Storage

As shown in Figure 6, the stability of the different microcapsules containing probiotics was evaluated during storage at temperatures of  $4^\circ\text{C}$  and  $25^\circ\text{C}$ . At  $4^\circ\text{C}$ , the viability of free bacteria was decreased from  $10.12 \pm 0.15$  log CFU/mL to  $5.96 \pm 0.27$ ,  $3.58 \pm 0.24$  and  $1.17 \pm 0.36$  log CFU/mL, after storage for 4 weeks, 8 weeks and 12 weeks, respectively. At  $25^\circ\text{C}$ , no free *Lactobacillus acidophilus* survived after 10 weeks of storage. The storage stability of *Lactobacillus acidophilus* was significantly ( $p < 0.05$ ) improved by encapsulation, especially in WPI-OSA-starch microcapsules. Bacterial vitality was maintained at  $9.22 \pm 0.31$  and  $6.25 \pm 0.36$  log CFU/g after 12 weeks of storage at  $4^\circ\text{C}$  and  $25^\circ\text{C}$ , respectively. Thus, it can be concluded that WPI-OSA-starch microcapsules can effectively protect *Lactobacillus acidophilus* during storage, mainly due to the smoother surface and the more compact structure of the microcapsules, as well as the relatively high hydrophobicity of OSA starch, which retards the diffusion of oxygen, moisture and other substances into the microcapsules during storage [1,43]. Similarly, the significantly ( $p < 0.05$ ) higher storage stability of probiotics in sodium-caseinate-gum-ghatti, sodium-caseinate-gum-arabic, soy-protein-isolate-peach-gum-polysaccharide and soy-protein-isolate-pectin microcapsules

than those in protein/polysaccharide-only microcapsules and free bacteria has also been reported [9,10,45].

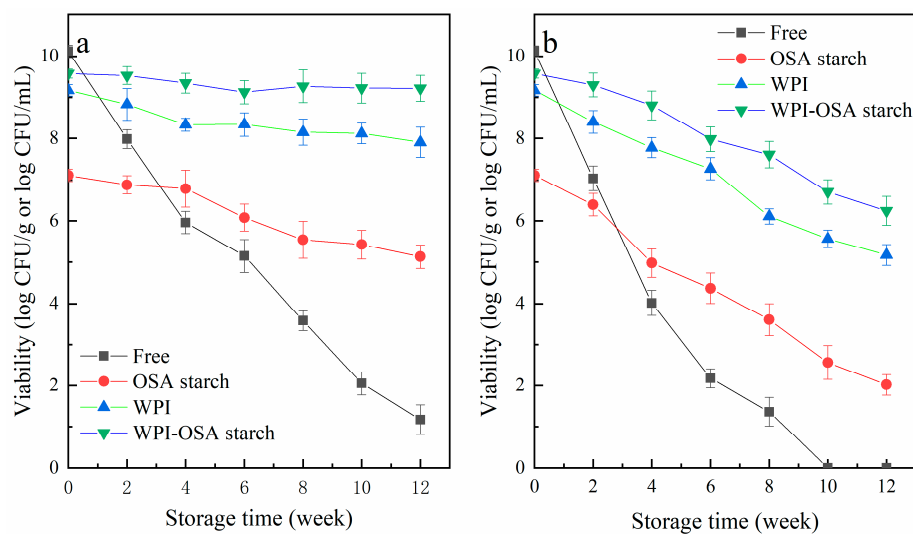


**Figure 6.** Viability of free and microencapsulated *Lactobacillus acidophilus* during storage at (a) 4 °C and (b) 25 °C.

### 3. Materials and Methods

#### 3.1. Material

*Lactobacillus acidophilus* 11073 was obtained from Gaofuji Biological Technology Co., Ltd. (Chengdu, China). Rice starch (amylose content of  $21.54 \pm 0.85\%$ ) was obtained from Haixi Biological Technology Co., Ltd. (Guangzhou, China). WPI was obtained from Haofa Biological Technology Co., Ltd. (Zhengzhou, China). De Man, Rogosa Sharp (MRS) agar and broth were obtained from Aoboxing Biological Technology Co., Ltd. (Beijing, China). OSA, pepsin (P7012), pancreatin (P7545), amyloglucosidase (A7095), porcine-bile extract (B8613) and rhodamine B isothiocyanate (RBITC) were obtained from Sigma-Aldrich (St. Louis, MO, USA). Other analytical pure chemical reagents were obtained from Cologne Chemical Co. (Chengdu, China).

#### 3.2. Synthesis of OSA Starch

OSA starch was synthesised following a previously reported process [46]. Briefly, 100 g of rice starch was mixed with 400 mL of distilled water. After adjusting the pH of the mixture to 8.5 with 1 M sodium hydroxide (NaOH) solution, 3 g of OSA was slowly added while keeping the pH at 8.5. After 6 h of reaction at 25 °C, the pH was lowered to 7.0 with 1 M hydrochloric acid (HCl) solution (1 M). The precipitate obtained via centrifugation was washed three times with distilled water and then once with acetone. The OSA starch obtained was dried to the initial moisture content of starch, ground to powder and then passed through a 100-mesh sieve.

#### 3.3. Complex Coacervation Formation and Characterisation

##### 3.3.1. Preparation of the WPI-OSA-Starch Solution

The preparation of WPI solution (1%, *w/v*) was performed by mixing the powder of WPI with aqua destillata and slowly stirring until complete hydration was achieved. The OSA-starch solution (1%, *w/v*) was prepared by mixing the powder of OSA starch with aqua destillata, followed by gelatinisation at 95 °C for 20 min. As the retrogradation usually occurred in gelatinised starch, the fresh OSA starch solution had to be prepared for each experiment and used immediately after preparation.

### 3.3.2. Turbidity Measurement

Turbidity measurements were performed at different ratios (WPI:OSA starch of 0:1, 0.5:1, 1:1, 2:1, 3:1 and 1:0) with a pH range of 2.0–6.5 using a UV-vis spectrophotometer (SDPTOP UV-2400, Shanghai, China) at 600 nm. In order to adapt the microencapsulation and keep the turbidity values in an appropriate range, measurements were made at a relatively high concentration (total biopolymer concentration of 0.2%, *w/v*), using the glass cells with an optical path of 0.5 cm [47]. The optimum pH (pH<sub>opt</sub>) was defined as the pH at which maximum turbidity was achieved [48].

### 3.3.3. Zeta Potential Analysis

The zeta potential of the solution of WPI, OSA starch and the mixture of them at different ratios (WPI:OSA starch of 0.5:1, 1:1, 2:1 and 3:1) was determined as a function of pH (3.0–6.5, adjusted with an HCl solution) using a zetasizer (Nano-ZS, Malvern Instruments, Ltd., Worcestershire, UK). The pH at which the zeta potential reaches 0 was defined to be the isoelectric point (IEP) [48].

### 3.3.4. Yield Measurement of Complex Coacervates

In order to study the adaptability of the process in the field of microencapsulation, the yields of WPI-OSA-starch-complex coacervates with different ratios (WPI:OSA starch of 0.5:1, 1:1, 2:1 and 3:1) and different total polymer concentrations (1% and 5%, *w/v*) were determined following the approach described by Carpentier et al. [48] and Chen et al. [47]. Briefly, the pH of each mixed solution of WPI-OSA starch was adjusted to its pH<sub>opt</sub>. When phase separation was evident, the liquid complex coacervates were collected via centrifugation (9000 × *g*, 20 min) and then dehydrated at 105 °C to constant mass. The yield of each complex coacervate was calculated according to Equation (1):

$$\text{Yield (\%)} = W_c / W_t \times 100 \quad (1)$$

In this equation,  $W_c$  is the dry weight of the complex coacervates (g) and  $W_t$  is the sum of the dry weight of WPI and OSA starch used for the complex coacervation (g).

## 3.4. Microencapsulation of Probiotic Bacteria

Glycerol-preserved *Lactobacillus acidophilus* was incubated in an MRS culture medium at 37 °C for 24 h to prepare *Lactobacillus acidophilus* inoculum, which was then transferred to MRS culture medium and incubated for a further 24 h. The bacterial suspension was centrifuged (6000 × *g*/5 min) and the pellet was washed twice and redispersed in sterile normal saline solution to give a final concentration of approximately 10<sup>10</sup> CFU/mL.

Microcapsules were prepared as follows: (1) prepare WPI, OSA starch and WPI-OSA-starch-mixed solution, the ratio and the total concentration were determined in Section 2.3; (2) keep the solution at 4 °C for 12 h to ensure adequate hydration; (2) add probiotic bacteria solution to the above solutions to about 10<sup>10</sup> CFU/g materials and stir continuously for 30 min; (3) adjust the pH to the pH<sub>opt</sub> determined in Section 2.3 and keep the above solutions at 4 °C for 12 h to ensure the completion of the complex coacervation; (4) dehydrate the complex coacervates containing the probiotic bacteria using a spray dryer (EYELA SD-1000, Tokyo Rikakikai, Ltd., Tokyo, Japan) with the following parameters: inlet/outlet temperature 120 °C/70 °C; gas flow rate 30 m<sup>3</sup>/h.

## 3.5. Characterisation of the Microcapsules

### 3.5.1. FTIR Spectroscopy

The FTIR spectrum of the different microcapsules containing probiotics was measured using an FTIR spectrometer (Nicolet iS10, Thermo Fisher Scientific, Ltd., Waltham, MA, USA). Briefly, 2 mg of microcapsule powder and 98 mg of KBr were blended and ground to a fine powder using an agate mortar. The ground powder was then pressed into transparent

flakes using a tablet press. The range of the wave number for measurement was set to 400–4000  $\text{cm}^{-1}$ . The spectral data were obtained via 32 scans with a resolution of 1  $\text{cm}^{-1}$ .

### 3.5.2. Fluorescence Microscopy

*Lactobacillus acidophilus* were labelled with RBITC according to the approach reported by Peñalva et al. [23]. Different microcapsules containing RBITC-labelled bacteria were prepared as described in Section 2.4 and analysed via an inverted fluorescence microscope (Nikon TS100, Tokyo, Japan).

### 3.5.3. Microstructure Observation

A scanning electron microscope (SEM) (SU8010, Hitachi Science Systems, Ltd., Tokyo, Japan) was used to measure the microstructure of the different microcapsules containing probiotics. After, they were placed on the adhesive carbon discs and coated with a gold layer. Images of each sample were obtained at 10.0 kV accelerating potential and 20,000 $\times$  magnification.

### 3.5.4. Water Content and Water Activity

The water content of the different microcapsules containing probiotics was measured by removing the water at 105 °C to constant mass. The water-activity meter (LabMas-terav., Lachen, Switzerland) was used to analyse the water activity ( $a_w$ ) of different microcapsules containing probiotics at 25 °C.

## 3.6. Determination of Microencapsulation Viability

Following the approach reported by Zhao et al. [49], microcapsules (dry weight) were dispersed in sterile normal saline solution at a ratio of 1:99 ( $w:v$ ), kept at 37 °C for 60 min and then vortexed to homo-dispersion. The suspension was then serially diluted and counted via the standard plate count (SPC) method using MRS agar. Incubation of the plates was performed at 37 °C for 2 days.

## 3.7. Viability under Different Treatments

### 3.7.1. SGI Digestion

The viability of free and microencapsulated probiotic bacteria after SGI digestion was determined following the approach described by Mao et al. [50], with some modifications. The sterilised sodium chloride (NaCl) solution (0.2%,  $w/v$ , pH 2.0) containing pepsin (0.3%,  $w/v$ ) was prepared and used as the simulated gastric fluid (SGF). The NaCl solution (0.2%,  $w/v$ , pH 8.0) containing pancreatin (0.1%,  $w/v$ ) and bile salts (0.3%,  $w/v$ ) was prepared and used as the simulated intestinal fluid (SIF). For SGI digestion, microcapsules (0.1 g) or free (0.1 mL) probiotic bacteria were added to 9.9 mL SGF and kept at 37 °C for 120 min. At 60 and 120 min, 0.1 mL of SGF was taken from each sample, serially diluted and counted via the SPC method. After simulated gastric digestion, the rest of SGF was moved to the SIF and the probiotic bacteria were counted at 60, 120, 180, 240, 300 and 360 min as previously described.

### 3.7.2. Thermal Treatment

To measure the thermal stability, microcapsules (1 g) or free (1 mL) probiotic bacteria were mixed with 9 mL sterile normal saline solution, and then incubated in a thermostat water bath (65 °C/30 min or 75 °C/10 min) followed by cooling with ice. The number of viable bacteria after thermal treatment was then determined.

### 3.7.3. Storage

To determine the storage stability, microcapsules (1 g) or free (1 mL) probiotic bacteria were preserved in sealed tubes at 4 °C/25 °C for 12 weeks. Each week, 0.1 mL of free bacteria or 0.1 g of microcapsules were taken from each sample and counted as previously described.

### 3.8. Statistical Analysis

Each measurement was performed three times and the data were recorded as the mean  $\pm$  standard deviation. Statistical differences between samples were analysed using SPSS software, with one-way analysis of variance (ANOVA) and Tukey's test ( $p < 0.05$ ).

## 4. Conclusions

In this study, complex coacervates of WPI and OSA starch were prepared for microencapsulation of *Lactobacillus acidophilus*. The optimum mixing ratio and pH for the preparation of the WPI-OSA-starch-complex coacervate were found to be 2:1 and 4.0, respectively. The occurrence of an electrostatic interaction between WPI and OSA starch in microcapsules was confirmed via FTIR. The spray-dried WPI-OSA starch microcapsules exhibited more compact structures and smoother surfaces than WPI-OSA starch-only microcapsules. Microencapsulation via the complex coacervation of WPI-OSA starch was found to be effective in improving the viability of *Lactobacillus acidophilus* during spray drying, SGI digestion, thermal treatment and long-term storage. Taken together, these results demonstrate that WPI-OSA-starch-complex coacervates are promising wall materials for probiotic encapsulation.

**Author Contributions:** Conceptualisation, Q.L., Q.B. and Y.Y. (Yongjun Yuan); methodology, Q.L. and S.W.; validation, C.L., X.Y. and S.W.; formal analysis, C.L., X.Y. and S.W.; investigation, C.L., S.W., Y.Y. (Yunting Yang), Y.L. and M.X. data curation, C.L., X.Y. and S.W.; writing—original draft preparation, C.L., X.Y. and Q.L.; writing—review and editing, Q.L. and Y.X.; visualisation, C.L. and X.Y.; supervision, Q.B. and Y.Y. (Yongjun Yuan); project administration, Q.B. and Y.Y. (Yongjun Yuan); funding acquisition, Q.L. All authors have read and agreed to the published version of the manuscript.

**Funding:** This research was funded by the Sichuan Science and Technology Program (2020YFN0092) and the Key Natural Science Foundation of Xihua University (Z17126).

**Institutional Review Board Statement:** Not applicable.

**Informed Consent Statement:** Not applicable.

**Data Availability Statement:** Data is contained within the article.

**Conflicts of Interest:** The authors declare no conflict of interest.

**Sample Availability:** Not available.

## References

1. Qi, X.; Lan, Y.; Ohm, J.; Chen, B.; Rao, J. The viability of complex coacervate encapsulated probiotics during simulated sequential gastrointestinal digestion affected by wall materials and drying methods. *Food Funct.* **2021**, *12*, 8907–8919. [[CrossRef](#)]
2. Kowalska, E.; Ziarno, M.; Ekielski, A.; Zelazinski, T. Materials Used for the Microencapsulation of Probiotic Bacteria in the Food Industry. *Molecules* **2022**, *27*, 3321. [[CrossRef](#)]
3. Gullifa, G.; Risoluti, R.; Mazzoni, C.; Barone, L.; Papa, E.; Battistini, A.; Martin Fraguas, R.; Materazzi, S. Microencapsulation by a Spray Drying Approach to Produce Innovative Probiotics-Based Products Extending the Shelf-Life in Non-Refrigerated Conditions. *Molecules* **2023**, *28*, 860. [[CrossRef](#)]
4. Guo, Q.; Li, S.; Tang, J.; Chang, S.; Qiang, L.; Du, G.; Yue, T.; Yuan, Y. Microencapsulation of *Lactobacillus plantarum* by spray drying: Protective effects during simulated food processing, gastrointestinal conditions, and in kefir. *Int. J. Biol. Macromol.* **2022**, *194*, 539–545. [[CrossRef](#)] [[PubMed](#)]
5. Paula, D.; Martins, E.; Costa, N.; de Oliveira, P.; de Oliveira, E.; Ramos, A. Use of gelatin and gum arabic for microencapsulation of probiotic cells from *Lactobacillus plantarum* by a dual process combining double emulsification followed by complex coacervation. *Int. J. Biol. Macromol.* **2019**, *133*, 722–731. [[CrossRef](#)] [[PubMed](#)]
6. da Silva, T.; de Deus, C.; de Souza Fonseca, B.; Lopes, E.; Cichoski, A.; Esmerino, E.; de Bona da Silva, C.; Muller, E.; Moraes Flores, E.; de Menezes, C. The effect of enzymatic crosslinking on the viability of probiotic bacteria (*Lactobacillus acidophilus*) encapsulated by complex coacervation. *Food Res. Int.* **2019**, *125*, 108577. [[CrossRef](#)]
7. Zhang, B.; Zheng, L.; Liang, S.; Lu, Y.; Zheng, J.; Zhang, G.; Li, W.; Jiang, H. Encapsulation of Capsaicin in Whey Protein and OSA-Modified Starch Using Spray-Drying: Physicochemical Properties and Its Stability. *Foods* **2022**, *11*, 612. [[CrossRef](#)] [[PubMed](#)]
8. Yao, M.; Xie, J.; Du, H.; McClements, D.J.; Xiao, H.; Li, L. Progress in microencapsulation of probiotics: A review. *Compr. Rev. Food Sci. Food Saf.* **2020**, *19*, 857–874. [[CrossRef](#)] [[PubMed](#)]

9. Hu, R.; Dong, D.; Hu, J.; Liu, H. Improved viability of probiotics encapsulated in soybean protein isolate matrix microcapsules by coacervation and cross-linking modification. *Food Hydrocoll.* **2023**, *138*, 108457. [\[CrossRef\]](#)
10. Yao, H.; Liu, B.; He, L.; Hu, J.; Liu, H. The incorporation of peach gum polysaccharide into soy protein based microparticles improves probiotic bacterial survival during simulated gastrointestinal digestion and storage. *Food Chem.* **2023**, *413*, 135596. [\[CrossRef\]](#)
11. Yuan, C.; Hu, R.; He, L.; Hu, J.; Liu, H. Extraction and prebiotic potential of  $\beta$ -glucan from highland barley and its application in probiotic microcapsules. *Food Hydrocoll.* **2023**, *139*, 108520. [\[CrossRef\]](#)
12. Diệp Huy Vũ, P.; Rodklongtan, A.; Chitprasert, P. Whey protein isolate-lignin complexes as encapsulating agents for enhanced survival during spray drying, storage, and in vitro gastrointestinal passage of *Lactobacillus reuteri* KUB-AC5. *LWT-Food Sci. Technol.* **2021**, *148*, 111725. [\[CrossRef\]](#)
13. Yin, M.; Yuan, Y.; Chen, M.; Liu, F.; Saqib, M.; Chiou, B.; Zhong, F. The dual effect of shellac on survival of spray-dried *Lactobacillus rhamnosus* GG microcapsules. *Food Chem.* **2022**, *389*, 132999. [\[CrossRef\]](#) [\[PubMed\]](#)
14. Guo, Y.; Qiao, D.; Zhao, S.; Zhang, B.; Xie, F. Starch-based materials encapsulating food ingredients: Recent advances in fabrication methods and applications. *Carbohydr. Polym.* **2021**, *270*, 118358. [\[CrossRef\]](#) [\[PubMed\]](#)
15. Dewi, A.; Santoso, U.; Pranoto, Y.; Marseno, D. Dual Modification of Sago Starch via Heat Moisture Treatment and Octenyl Succinylation to Improve Starch Hydrophobicity. *Polymers* **2022**, *14*, 1086. [\[CrossRef\]](#) [\[PubMed\]](#)
16. Zhou, F.; Dong, M.; Huang, J.; Lin, G.; Liang, J.; Deng, S.; Gu, C.; Yang, Q. Preparation and Physico-Chemical Characterization of OSA-Modified Starches from Different Botanical Origins and Study on the Properties of Pickering Emulsions Stabilized by These Starches. *Polymers* **2023**, *15*, 706. [\[CrossRef\]](#)
17. Yao, T.; Wen, Y.; Xu, Z.; Ma, M.; Li, P.; Brennan, C.; Sui, Z.; Corke, H. Octenylsuccinylation differentially modifies the physico-chemical properties and digestibility of small granule starches. *Int. J. Biol. Macromol.* **2020**, *144*, 705–714. [\[CrossRef\]](#)
18. Wang, F.; Yang, R.; Wang, J.; Wang, A.; Li, M.; Wang, R.; Strappe, P.; Zhou, Z. Starch propionylation acts as novel encapsulant for probiotic bacteria: A structural and functional analysis. *Int. J. Biol. Macromol.* **2022**, *213*, 11–18. [\[CrossRef\]](#)
19. Cruz-Benítez, M.; Gómez-Aldapa, C.; Castro-Rosas, J.; Hernández-Hernández, E.; Gómez-Hernández, E.; Fonseca-Florido, H. Effect of amylose content and chemical modification of cassava starch on the microencapsulation of *Lactobacillus pentosus*. *LWT-Food Sci. Technol.* **2019**, *105*, 110–117. [\[CrossRef\]](#)
20. Wang, Y.; Zheng, Z.; Wang, K.; Tang, C.; Liu, Y.; Li, J. Prebiotic carbohydrates: Effect on physicochemical stability and solubility of algal oil nanoparticles. *Carbohydr. Polym.* **2020**, *228*, 115372. [\[CrossRef\]](#)
21. Sharifi, S.; Rezazad-Bari, M.; Alizadeh, M.; Almasi, H.; Amiri, S. Use of whey protein isolate and gum Arabic for the co-encapsulation of probiotic *Lactobacillus plantarum* and phytosterols by complex coacervation: Enhanced viability of probiotic in Iranian white cheese. *Food Hydrocoll.* **2021**, *113*, 106496. [\[CrossRef\]](#)
22. Mao, L.; Pan, Q.; Yuan, F.; Gao, Y. Formation of soy protein isolate-carrageenan complex coacervates for improved viability of *Bifidobacterium longum* during pasteurization and in vitro digestion. *Food Chem.* **2019**, *276*, 307–314. [\[CrossRef\]](#) [\[PubMed\]](#)
23. Peñalva, R.; Martínez-López, A.; Gamazo, C.; Gonzalez-Navarro, C.; González-Ferrero, C.; Virto-Resano, R.; Brotons-Canto, A.; Vitas, A.; Collantes, M.; Peñuelas, I.; et al. Encapsulation of *Lactobacillus plantarum* in casein-chitosan microparticles facilitates the arrival to the colon and develops an immunomodulatory effect. *Food Hydrocoll.* **2022**, *136*, 108213. [\[CrossRef\]](#)
24. Zhang, J.; Jia, G.; Wanbin, Z.; Minghao, J.; Wei, Y.; Hao, J.; Liu, X.; Gan, Z.; Sun, A. Nanoencapsulation of zeaxanthin extracted from *Lycium barbarum* L. by complex coacervation with gelatin and CMC. *Food Hydrocoll.* **2021**, *112*, 10628. [\[CrossRef\]](#)
25. Qiu, L.; Zhang, M.; Adhikari, B.; Chang, L. Microencapsulation of rose essential oil in mung bean protein isolate-apricot peel pectin complex coacervates and characterization of microcapsules. *Food Hydrocoll.* **2022**, *124*, 107366. [\[CrossRef\]](#)
26. Tian, L.; Roos, Y.; Miao, S. Phase behavior and complex coacervation of whey protein isolate-*Tremella fuciformis* polysaccharide solution. *Food Hydrocoll.* **2023**, *143*, 108871. [\[CrossRef\]](#)
27. Plati, F.; Ritzoulis, C.; Pavlidou, E.; Paraskevopoulou, A. Complex coacervate formation between hemp protein isolate and gum Arabic: Formulation and characterization. *Int. J. Biol. Macromol.* **2021**, *182*, 144–153. [\[CrossRef\]](#)
28. Zhao, Y.; Khalid, N.; Shu, G.; Neves, M.A.; Kobayashi, I.; Nakajima, M. Complex coacervates from gelatin and octenyl succinic anhydride modified kudzu starch: Insights of formulation and characterization. *Food Hydrocoll.* **2019**, *86*, 70–77. [\[CrossRef\]](#)
29. Lan, Y.; Ohm, J.; Chen, B.; Rao, J. Phase behavior and complex coacervation of concentrated pea protein isolate-beet pectin solution. *Food Chem.* **2020**, *307*, 125536. [\[CrossRef\]](#)
30. Ghadermazi, R.; Khosrowshahi Asl, A.; Tamjidi, F. Complexation and coacervation of whey protein isolate with quince seed mucilage. *J. Disper. Sci. Technol.* **2020**, *42*, 2032–2041. [\[CrossRef\]](#)
31. Chen, K.; Zhang, M.; Adhikari, B.; Wang, M. Microencapsulation of Sichuan pepper essential oil in soybean protein isolate-Sichuan pepper seed soluble dietary fiber complex coacervates. *Food Hydrocoll.* **2022**, *125*, 107421. [\[CrossRef\]](#)
32. Liu, J.; Shim, Y.; Shen, J.; Wang, Y.; Reaney, M. Whey protein isolate and flaxseed (*Linum usitatissimum* L.) gum electrostatic coacervates: Turbidity and rheology. *Food Hydrocoll.* **2017**, *64*, 18–27. [\[CrossRef\]](#)
33. Ghadermazi, R.; Khosrowshahi Asl, A.; Tamjidi, F. Optimization of whey protein isolate-quince seed mucilage complex coacervation. *Int. J. Biol. Macromol.* **2019**, *131*, 368–377. [\[CrossRef\]](#)
34. Timilsena, Y.; Wang, B.; Adhikari, R.; Adhikari, B. Preparation and characterization of chia seed protein isolate–chia seed gum complex coacervates. *Food Hydrocoll.* **2016**, *52*, 554–563. [\[CrossRef\]](#)

35. Bhargavi, N.; Dhathathreyan, A.; Sreeram, K. Design of pH-Induced complex coacervates of gelatin and wattle. *Colloids Surf. Physicochem. Eng. Asp.* **2020**, *602*, 125148. [[CrossRef](#)]
36. Liu, Q.; Cui, H.; Muhoza, B.; Hayat, K.; Hussain, S.; Tahir, M.U.; Zhang, X.; Ho, C. Whey protein isolate-dextran conjugates: Decisive role of glycation time dependent conjugation degree in size control and stability improvement of colloidal nanoparticles. *LWT-Food Sci. Technol.* **2021**, *148*, 111766. [[CrossRef](#)]
37. Xu, T.; Jiang, C.; Zhou, Q.; Gu, Z.; Cheng, L.; Tong, Y.; Hong, Y. Complexation behavior of octenyl succinic anhydride starch with chitosan. *Food Hydrocoll.* **2021**, *119*, 109350. [[CrossRef](#)]
38. Naderi, B.; Keramat, J.; Nasirpour, A.; Aminifar, M. Complex coacervation between oak protein isolate and gum Arabic: Optimization & functional characterization. *Int. J. Food Prop.* **2020**, *23*, 1854–1873.
39. Zhang, J.; Du, H.; Ma, N.; Zhong, L.; Ma, G.; Pei, F.; Chen, H.; Hu, Q. Effect of ionic strength and mixing ratio on complex coacervation of soy protein isolate/*Flammulina velutipes* polysaccharide. *Food Sci. Hum. Well* **2023**, *12*, 183–191. [[CrossRef](#)]
40. Jiang, J.; Ma, C.; Song, X.; Zeng, J.; Zhang, L.; Gong, P. Spray drying co-encapsulation of lactic acid bacteria and lipids: A review. *Trends Food Sci. Technol.* **2022**, *129*, 134–143. [[CrossRef](#)]
41. Bora, A.F.M.; Kouame, K.J.E.; Li, X.; Liu, L.; Sun, Y.; Ma, Q.; Liu, Y. Development, characterization and probiotic encapsulating ability of novel *Momordica charantia* bioactive polysaccharides/whey protein isolate composite gels. *Int. J. Biol. Macromol.* **2023**, *225*, 454–466. [[CrossRef](#)] [[PubMed](#)]
42. Liu, Z.; Shi, A.; Wu, C.; Hei, X.; Li, S.; Liu, H.; Jiao, B.; Adhikari, B.; Wang, Q. Natural Amphiphilic Shellac Nanoparticle-Stabilized Novel Pickering Emulsions with Droplets and Bi-continuous Structures. *ACS Appl. Mater Interfaces* **2022**, *14*, 57350–57361. [[CrossRef](#)]
43. Zhao, M.; Huang, X.; Zhang, H.; Zhang, Y.; Gänzle, M.; Yang, N.; Nishinari, K.; Fang, Y. Probiotic encapsulation in water-in-water emulsion via heteroprotein complex coacervation of type-A gelatin/sodium caseinate. *Food Hydrocoll.* **2020**, *105*, 105790. [[CrossRef](#)]
44. Huang, X.; Ganzle, M.; Zhang, H.; Zhao, M.; Fang, Y.; Nishinari, K. Microencapsulation of probiotic lactobacilli with shellac as moisture barrier and to allow controlled release. *J. Sci. Food Agric.* **2021**, *101*, 726–734. [[CrossRef](#)] [[PubMed](#)]
45. Liu, H.; Gong, J.; Chabot, D.; Miller, S.S.; Cui, S.W.; Ma, J.; Zhong, F.; Wang, Q. Incorporation of polysaccharides into sodium caseinate-low melting point fat microparticles improves probiotic bacterial survival during simulated gastrointestinal digestion and storage. *Food Hydrocoll.* **2016**, *54*, 328–337. [[CrossRef](#)]
46. Zhang, W.; Cheng, B.; Li, J.; Shu, Z.; Wang, P.; Zeng, X. Structure and Properties of Octenyl Succinic Anhydride-Modified High-Amylose Japonica Rice Starches. *Polymers* **2021**, *13*, 1325. [[CrossRef](#)]
47. Carpentier, J.; Conforto, E.; Chaigneau, C.; Vendeville, J.; Maugard, T. Complex coacervation of pea protein isolate and tragacanth gum: Comparative study with commercial polysaccharides. *Innov. Food Sci. Emerg.* **2021**, *69*, 102641. [[CrossRef](#)]
48. Chen, K.; Zhang, M.; Mujumdar, A.S.; Wang, H. Quinoa protein-gum Arabic complex coacervates as a novel carrier for eugenol: Preparation, characterization and application for minced pork preservation. *Food Hydrocoll.* **2021**, *120*, 106915. [[CrossRef](#)]
49. Zhao, M.; Wang, Y.; Huang, X.; Gaenzle, M.; Wu, Z.; Nishinari, K.; Yang, N.; Fang, Y. Ambient storage of microencapsulated *Lactobacillus plantarum* ST-III by complex coacervation of type-A gelatin and gum arabic. *Food Funct.* **2018**, *9*, 1000–1008. [[CrossRef](#)]
50. Mao, L.; Pan, Q.; Hou, Z.; Yuan, F.; Gao, Y. Development of soy protein isolate-carrageenan conjugates through Maillard reaction for the microencapsulation of *Bifidobacterium longum*. *Food Hydrocoll.* **2018**, *84*, 489–497. [[CrossRef](#)]

**Disclaimer/Publisher’s Note:** The statements, opinions and data contained in all publications are solely those of the individual author(s) and contributor(s) and not of MDPI and/or the editor(s). MDPI and/or the editor(s) disclaim responsibility for any injury to people or property resulting from any ideas, methods, instructions or products referred to in the content.